J MATER RES TECHNOL. 2020;9(6):12723–12736

Available online at www.sciencedirect.com

jmr&t Journal of Materials Research and Technology

https://www.journals.elsevier.com/journal-of-materials-research-and-technology

Original Article

Glass fabric reinforced polybenzoxazine composites filled with nanosilica: A High impact response poises use as strike panels in multilayered armor applications

Phattarin Mora[a], *Manunya Okhawilai*[b], *Chanchira Jubsilp*[c], *Christopher W. Bielawski*[a,d,e], *Sarawut Rimdusit*[a,f,*]

[a] *Polymer Engineering Laboratory, Department of Chemical Engineering, Faculty of Engineering, Chulalongkorn University, Bangkok 10330, Thailand*

[b] *Metallurgy and Materials Science Research Institute, Chulalongkorn University, Bangkok 10330, Thailand*

[c] *Department of Chemical Engineering, Faculty of Engineering, Srinakharinwirot University, Nakhonnayok 26120, Thailand*

[d] *Center for Multidimensional Carbon Materials (CMCM), Institute for Basic Science (IBS), Ulsan 44919, Republic of Korea*

[e] *Department of Chemistry, Ulsan National Institute of Science and Technology (UNIST), Ulsan 44919, Republic of Korea*

[f] *Research Unit in Polymeric Materials for Medical Practice Devices, Department of Chemical Engineering, Faculty of Engineering, Chulalongkorn University, Bangkok, Thailand*

ARTICLE INFO

Article history:
Received 13 May 2020
Accepted 2 September 2020

Keywords:
Polybenzoxazine
Nanocomposite
Nanosilica
Numerical simulation
Multilayered armor.

ABSTRACT

Glass fabric reinforced polybenzoxazine-based composites filled with nanosilica (nano-SiO_2) particles were used to create strike panels for multilayered armor applications. The effect of the added nano-SiO_2 on the mechanical properties and ballistic impact responses of the composites was quantified using a variety of techniques and related to the interfacial interactions between the two materials. Impact response was effectively mitigated by the added nano-SiO_2 as composite panels which contained the additive exhibited smaller damage areas as well as lower penetration depths after being subjected to 5.56 × 45 mm projectiles when compared to composite panels that lacked the additive. Furthermore, a series of numerical simulations predicted that composites of appropriate thickness should protect against the penetration of projectiles with velocities of 930 ± 20 m/s and ballistic limit velocities as high as 1075 m/s. Collectively, these results indicate that the composites may be used as strike panels in ballistic armor applications.

* *Corresponding author.*
E-mail: Sarawut.R@chula.ac.th (S. Rimdusit).

https://doi.org/10.1016/j.jmrt.2020.09.005

1. Introduction

Novel projectiles with increasing size, shape and/or kinetic energy significantly increases the level of threat which has prompted the development of materials for use in high performance ballistic armor applications [1–5]. The National Institute of Justice (NIJ) standard is often used in ballistic impact tests to evaluate personal protection. The standard requires that the armor stop the projectile in a clay witness with a penetration depth of less than or equal to 44 mm [6,7]. According to the NIJ standard, multilayered hard armor should protect against the perforation of 5.56 mm × 45 mm projectiles (SS109) which is one of the most powerful projectiles with the perforated steel core for armor piercing at high impact velocities [8]. Multilayered hard armor typically consists of a strike panel and a back panel. The strike panel is necessary to break up and destroy the projectile tip while the back panel absorbs the kinetic energy of the projectile [9,10]. The back panel is typically a reinforced polymer composite and the strike panel is made of alumina (Al_2O_3) [11,12], boron carbide (B_4C) [13,14], or silicon carbide (SiC) [15,16] ceramic tile. Since ceramics are heavy, brittle and can fail after an impact due to crack propagation [17], high-performance, light weight fiber reinforced polymer (FRP) composites have been developed as alternatives. Potential reinforcing fibers for use in such applications include aramid fibers [18–20], ultra-high molecular weight polyethylene fibers (UHMWPE) [21,22], glass fibers [23,24], and carbon fibers [25]. Glass fiber-reinforced composites may be ideal as they are relatively inexpensive and display suitable strength and stiffness properties.

An important factor that influences the ballistic performance displayed by FRP composites is the type of polymer matrix utilized as it effectively binds all of the reinforcement components together. The polybenzoxazines are a relatively new type of polymer matrix that are related to phenolic resins yet prepared through a ring-opening polymerization that does not require catalysts or curing agents and proceeds without the formation of by-products [26–28]. Polybenzoxazines exhibit a number of superior characteristics, including high dimensional stability, near-zero volumetric shrinkage and low water absorption [29]. Moreover, benzoxazine resins feature pendant phenol groups which can facilitate interactions with other fibers or fillers, or further modified with other chemical reagents, resins or polymers [30,31], and thus tailored to meet ballistic protection requirements. Gopinath et al. [32] reported that the interaction between the polymer matrix and reinforcing components was also an important factor that affects impact response, particularly in polymer composites that contained yarns [32].

The impact performance of strike panels that were comprised of glass fiber reinforced polybenzoxazine composites was previously investigated by Okhawilai et al. [33]. The panels were manufactured from either E-glass or S-glass fiber reinforced polybenzoxazines and backed by aramid fiber reinforced composites, and then subjected to 7.62 mm × 51 mm rifle projectiles at velocities of 847 ± 9.1 m/s. Panels comprised of S-glass displayed less damage and lower penetration depths than the E-glass analogues. The high tensile moduli of the strike panels could result in a superior ballistic impact response particularly in terms reducing back face deformation and penetration depth. Moreover, the hardness of the strike panel may reflect an ability to destroy the projectile into fragments and proceed without failure of the back panel. Regardless, the result demonstrated that S-glass fiber reinforced polybenzoxazine-based composites may be used as strike panels in hard ballistic armor applications.

FRP composites with optimal mechanical properties may be realized by balanced interactions between the polymer matrix and the fiber. One way to achieve such balance is through the incorporation of nanoparticles, such as nanosilica (nano-SiO_2) [34–36], carbon nanotubes (CNTs) [36,37] and/or nanoclays [38,39]. Zare and Rhee [40] investigated how adding carbon nanotubes (CNTs) to polymer matrices of polymer nanocomposites affected modulus predicted by numerical models. As a part of these efforts, it was discovered that the incorporation of nanoparticles could enhance the tensile modulus of the nanocomposites due to the interfacial bonding between polymer matrices and nanoparticles. Similarly, He et al. [41] studied the effects of added nanosilica on the properties of epoxy-based composites. The results showed that the key mechanical properties displayed by the composites, such as flexural strength, fracture toughness, and hardness, exhibited relatively high values when the added silica content reached 15 wt%. The enhancement may be due to an improvement in the wettability between the matrix and the added filler which ultimately increased the bonding interaction between the two components. Dueramae et al. [42] also investigated the effect of added nanosilica on the mechanical and thermal properties displayed by polybenzoxazine-based composites. The storage modulus and hardness of the composites increased by up to 83% and 49%, respectively, when compared to a virgin polybenzoxazine, and depending on how much nanosilica was added (up to 30 wt%).

An important parameter that is often encountered while studying penetration mechanics is the ballistic limit velocity, which refers to a critical velocity below which a projectile is capable of perforating the armor. Many efforts examined the relationships between impact velocity and residual velocity of the projectile on the ballistic limit velocity for a variety of materials [43–45]. Due to the complex ballistic penetration process, numerical simulations are often used to predict the ballistic performance. Ansari et al. [23] studied the perforation characteristics of unidirectional glass fiber reinforced laminates in part by considering different projectile nose shapes, impact velocities, impact angles and laminate thickness. A three dimensional finite element model was developed using Lagrangian functions and good correlation with the corresponding experimental data was realized. Likewise, Miranda et al. [44] studied the size of damage area in alumina plates that were impacted by cylindrical projectiles at various velocities. Finite elements modeling (FEM) was used to evaluated the ballistic performance and shapes of the materials. Good agreement between the experimental results and the model was observed and a number of simulations were conducted to predict the ballistic response.

Herein the effect of nanosilica on the mechanical properties and ballistic performance displayed by S-glass fabric reinforced polybenzoxazine composites was studied. The impact response, i.e. back face deformation and depth of pene-

tration, was evaluated and compared to analogues that lacked the nanosilica filler. Ballistic limit velocity and damage patterns were modeled using a series of numerical simulations. The focus of the present study is to develop the materials based on nanosilica-filled polybenzoxazine nanocomposites using as a novel strike panel impacted by a rigid 5.56 × 45 mm projectile (SS109) with high impact velocities to overcome the crack propagation of conventional materials.

2. Materials and preparation

2.1. Materials

Benzoxazine resins based on bisphenol-A, formaldehyde, and aniline (BA-a) were used as the polymer matrix. The bisphenol-A (polycarbonate grade) was kindly supplied by the Thai Polycarbonate Co., Ltd. (Rayong, Thailand). Formaldehyde (AR grade) and aniline (AR grade) were purchased from Merck Co., Ltd. and Panreac Quimica, S.A., respectively. A urethane prepolymer with a number average molecular weight (M_n) of 2000 g/mol was synthesized by combining 2,4-toluene diisocyanate (TDI) and propylene glycol (PPG). TDI and PPG were supplied by the South City Group (Thailand) and TPI Polyol Co., Ltd (Thailand), respectively. S-Glass fabrics (plain weave) and an aramid fabric with areal densities of 800 and 360 g/cm^2, respectively, were purchased from Thai Polyadd Limited Partnership (Thailand). Nano-SiO_2 (Reolosil_QS-20) was a product of Tokuyama Co., Tokyo, Japan. The nano-SiO_2 is amorphous white powder with fluffy characteristics and has a density of 2.203 g/cm^3. The average diameter of the primary filler particles ranged from 5 to 50 nm and displayed an average specific surface area of ~200 m^2/g. Multiwalled CNTs (MWCNTs) with an outer diameter of 12.9 nm and tube lengths of 3 – 12 μm were purchased from Nano Generation Co., Ltd. The density of the MWCNTs used in this study was 1.90 g/cm^3. All chemicals were used as received.

2.2. Resin preparation

The polybenzoxazine (BA-a) resin was synthesized from bisphenol A, formaldehyde, and aniline in a molar ratio of 1:4:2 based using the solvent-less synthesis technique [46]. The three reactants were continuously stirred at 110 °C for approximately 40 min. The obtained resin was in clear yellowish color and solid at room temperature. The solid resin was then ground into a fine powder. A urethane prepolymer was separately prepared from TDI and PPG (2000 Da) at a molar ratio of 2:1. The two reactants were directly mixed in a four-necked round-bottomed flask under a stream of nitrogen at a temperature of 70 °C for 2 h to yield a light yellow material. The urethane prepolymer was collected and kept in a closed container under nitrogen and stored at a cool temperature.

2.3. Sample preparation

The samples used in this study consisted of a strike panel and a back panel. The strike panel was fabricated from S-glass fabric reinforced poly(BA-a) composite filled with nano-SiO_2. The composite was prepared by the addition of nano-SiO_2 (0.0, 0.5, 1.0, 1.5, or 2.0 wt%) into the poly(BA-a). The nano-SiO_2 was first dried at 80 °C in an air-circulated oven for 24 h until a constant weight was measured. Afterward, the dried nano-SiO_2 was gently added and then mixed with the BA-a resin at 110 °C for 20 min to obtain a well dispersed mold. The specimen compositions are listed in Table 1. The mold was coated onto the S-glass fabric using the hand-layup technique at 120 °C to yield the prepregs. The prepregs were stacked and preheated at 180 °C for 20 min, 200 °C for 10 min and fully cured at 200 °C for 2 h under compression at a pressure of 15 MPa. The back panel was prepared from of an aramid fabric (80 wt%) reinforced polybenzoxazine/urethane (poly(BA-a/PU)) composite. To prepare the composites, BA-a was mixed with a urethane prepolymer (20 wt%). In some cases, the mixture was charged with MWCNTs (0.25 wt%) and then stirred at 110 °C for 20 min under the components were well dispersed. (Note: the MWCNTs were dried at 80 °C in an air-circulated oven for 24 h until a constant weight was achieved.) The resulting molds were coated on aramid fabrics using the hand-layup technique at 120 °C to yield the corresponding prepregs. The prepregs containing MWCNTs (10-ply) were stacked on the aramid fabric reinforced poly(BA-a/PU) composite (25-ply) and then heated 160 °C for 40 min, 180 °C for 20 min, and 200 °C for 10 min. The stack was then compressed under a pressure of 10 MPa and heated to 200 °C for 2 h. All samples were air-cooled to room temperature and then cut with a diamond blade into desired shapes.

Table 1 – Summary of starting materials used to prepare various composites.

Nano-SiO_2 (wt%)	BA-a (wt%)	S-glass fabric (wt%)
0.0	20.0	80.0
0.5	19.5	80.0
1.0	19.0	80.0
1.5	18.5	80.0
2.0	18.0	80.0

2.4. Characterization

2.4.1. Fourier transform infrared spectroscopy (FTIR)

Fourier transform infrared spectra were recorded using a Perkin-Elmer Spectrum GX FTIR spectrometer equipped with an ATR accessory. All spectra were taken with 64 scans at a resolution of 4 cm^{-1} and a spectral range of 4000–400 cm^{-1}.

2.4.2. Tensile properties of the samples

The tensile properties of 8-ply S-glass fabric reinforced poly(BA-a) composites filled with nano-SiO_2 (0.0–2.0 wt%) were evaluated according to the ASTM D3039 standard. Specimen dimensions were 130 × 25 × 3 mm^3. Tensile specimens were 10 mm in diameter and exhibited a 70 mm gage length. The length of the grip section was 27.5 mm. A universal testing machine (Instron Co., Ltd., model 8872) was used with a crosshead speed of 2 mm/min. A minimum of eight samples were tested and the results obtained from the measurements were averaged.

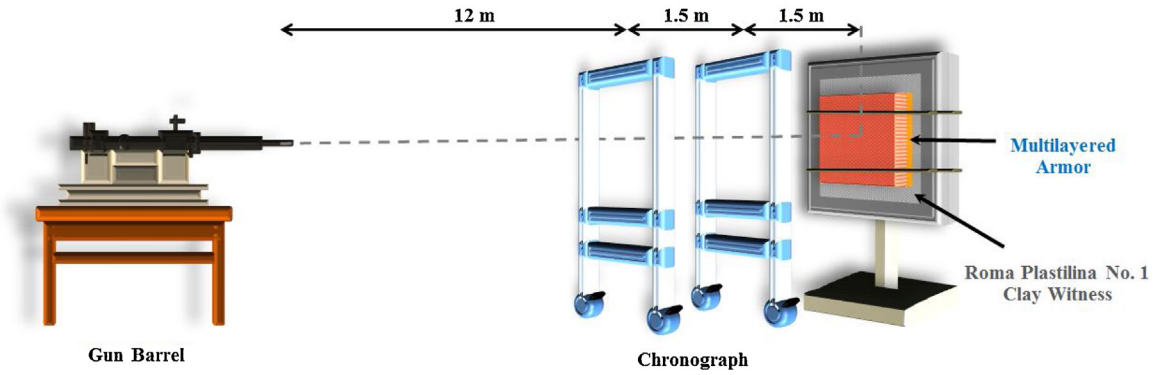

Fig. 1 – Schematic of the experimental setup used for the high velocity impact tests.

2.4.3. *Microhardness values of the samples*

The microhardness of an 8-ply S-glass fabric reinforced poly(BA-a) composite filled with nano-SiO_2 was studied using a Vickers hardness tester (Future-Tech Corp., model FM-700). A constant load of 500 gf (4.9 N) and a dwell time of 15 s were set. The diagonal length of the indentation was measured via a micrometric eyepiece coupled with a 50× objective lens. Averages of eight separate readings were reported.

2.4.4. *Morphologies of the samples*

Sample morphology was studied using a scanning electron microscope (SEM, model JSM-6510A from JEOL Ltd., Tokyo Japan) operating at an acceleration voltage of 15 kV. All samples were first coated with a thin layer of gold using a sputter coater (model SCD 040 from Oerlikon Balzers Coating (Thailand) Co. Ltd., Chonburi, Thailand) prior to imaging.

2.4.5. *Ballistic performance of the samples*

The ballistic impact tests were conducted using cartridges designed to propel projectiles in predetermined directions. A chronograph was placed in front of the multilayered armor holding unit to record the impact velocity of the projectiles. The experimental set-up is shown in Fig. 1. A $150 \times 150\,mm^2$ composite plate was clamped in front of a Roma Plastilina No. 1 Clay witness. The tests were conducted using 5.56×45 mm projectiles that proceeded with velocities of 920 ± 30 m/s and impacted the witnesses normal to their primary planes. The projectiles were measured to have a mass of 4.0 g. The depth of penetration after each impact was also measured.

2.4.6. *Numerical simulations of ballistic characteristics*

A series of numerical simulation were used to assess and predict the damage patterns and ballistic management characteristics of the composite materials. Multilayered armor composites that consisted of a strike panel and back panel were assembled. The strike panel made from a S-glass fabric reinforced poly(BA-a) composite filled with nano-SiO_2 was placed in front of the back panel. Previous results demonstrated that hybrid aramid composite panels consisting of 10-ply aramid fabric reinforced poly(BA-a/PU) composites filled with MWCNTs and stacked with a 25-ply fabric reinforced poly(BA-a/PU) composite exhibit appropriate energy absorption properties and thus are suitable for use as back panels [47]. As such, similar back panels were used herein. The ballistic limit and armor deformation were evaluated numerically with the ANSYS AUTODYN software package. Fiber reinforced polybenzoxazine composites were simulated as an orthotropic material in which the material properties differed along the three orthogonal planes. The orthotropic equation of state (EOS) allows a nonlinear function to be used in conjunction with the orthotropic stiffness matrix. Due to the nature of FRP composites, the fabric reinforced composite laminates with plain weave patterns were assumed to have identical properties in the fiber directions but different properties in other directions. It was also assumed that materials were homogeneous. The ballistic panel model was created with four fixed edges. A 5.56×45 mm projectile made of a copper jacket with a lead core and steel head was modeled using the strength models of Johnson-Cook and Steinberg-Guinan. The material properties of the projectile were obtained from the standard ANSYS AUTODYN material library [48] and are summarized in Table 2. The geometry of the projectile and the composite panel are shown in Fig. 2.

The simulations were performed under the same conditions as those described in the experimental section to facilitate comparison. In order to validate the input properties of the materials, experimental and simulated panel deformations were compared. Moreover, the deformation patterns of hard ballistic armor composite panels having dimensions of $150 \times 150\,mm^2$ were deduced from the simulated ballistic impacts. The V_{50} of the composite system, which may be defined as the incident impact velocity at which there is 50% probability of partial penetration and 50% probability of perforation, was numerically estimated from ballistic panel. The ballistic limit was determined by varying the impact velocities of the projectiles until the sample was perforated. The reported V_{50} was the average value of the highest partial penetration velocities and the lowest complete penetration velocities. The estimated energy absorption of the hard armor composites was calculated according to Eq. (1).

$$E_{Abs} = 1/2 m_p {V_{50}}^2 \quad (1)$$

where E_{Abs} is energy absorption (J), m_p is mass of projectile =0.004 kg [8] and V_{50} is ballistic limit velocity (m/s).

Table 2 – A summary of the properties of the materials used in 5.56 × 45 mm projectiles.

Material: Copper jacket	Value	Properties	Value	Properties	Value
Density	8450 kg m^{-1}	Gruneisen coefficient	2.04	Parameter S1	1.434
Shear modulus	3000 MPa	Parameter C1	3726 m/s	Failure	
Material: Lead head	Value	Properties	Value	Properties	Value
Density	11,340 kg m^{-1}	Derivative dG/dP	1	Parameter quadratic S2	0 s/m
Shear modulus	8600 MPa	Derivative dG/dT	-9.976 MPa/◦C	Failure	
Plasticity	Steinberg Guinan Strength	Derivative dY/dP	0.0,009,304	Maximum equivalent plastic strain	2
Initial yield stress	8 MPa	Parameter C1	2006 m/s	Melting temperature	760 K
Hardening constant	110	Parameter S1	1.429	Gruneisen coefficient	2.74
Material: Steel core	Value	Properties	Value	Properties	Value
Density	7830 kg m^{-1}	Shear modulus	8180 MPa	Melting temperature	1793 K
Bulk modulus	15,900 MPa	Yield stress	792 MPa	Reference strain rate	1
Ref. temperature	295.15 K	Hardening constant	792 MPa	Strain rate correction	1st order
Specific heat	477 J kg^{-1} K^{-1}	Hardening exponent	0.26		
Strength	Johnson-Cook	Strain rate constant	0.014		

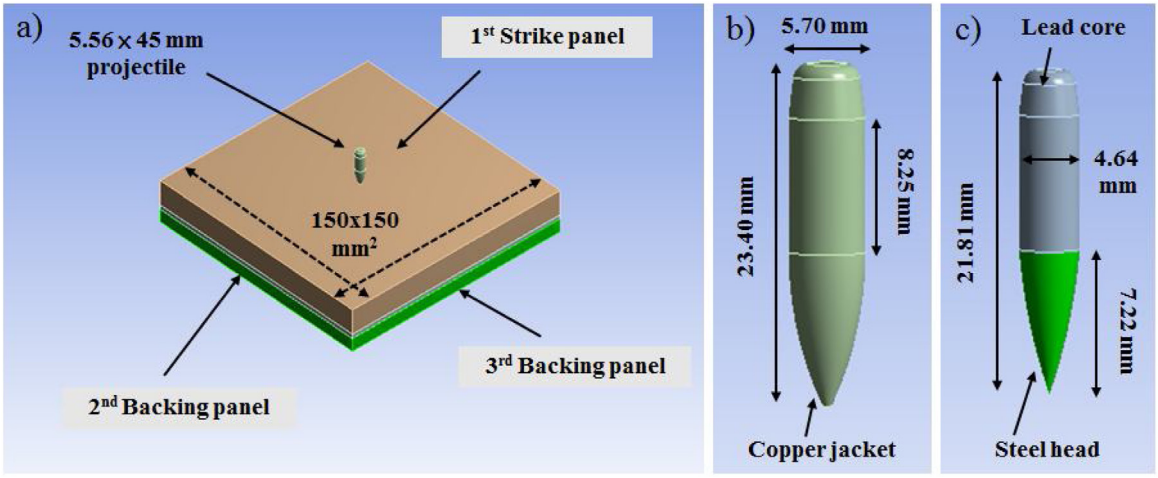

Fig. 2 – Dimensions of (a) the composite panel, (b) the jacket of the projectile and (c) the core and head of the projectile.

3. Results and discussion

3.1. *Spectroscopic investigation of poly(BA-a) composites filled with nano-SiO_2*

The chemical structures of the poly(BA-a) composites filled with nanosilica particles as well as their components were investigated by FT-IR spectroscopy. As shown in Fig. 3(a), a band at 1110 cm^{-1} was observed upon analysis of the nanosilica particles and assigned to the asymmetric stretching vibrations of the siloxane group (Si–O–Si). Absorptions at 810 cm^{-1} and 3425 cm^{-1} were also observed and attributed to the symmetric stretching of the Si–O–Si groups and symmetric stretching of hydroxyl groups, respectively. The identification of hydroxyl groups indicated that the nanosilica particles may be hydrophilic surface. As shown in Fig. 3(b), the IR spectrum recorded for the BA-a resin revealed a characteristic signal at 1230 cm^{-1} which was attributed to the oxazine ring. While the resin exhibited absorptions at 936 cm^{-1} and 1488 cm^{-1} which are characteristic of substituted arenes, the signals disappeared upon polymerization consistent with a ring-opening reaction as shown in Fig. 4. The disappearance was concomitant with the absorption of a tetra-substituted arene as new signals were observed at 878 cm^{-1} and 1477 cm^{-1}; see Fig. 3(c). Oxazine ring-opening was expected to afford a phenol which was confirmed from the appearance of a broad signal at 3380 cm^{-1}. The network formed between the poly(BA-a) and the nanosilica particles was also evaluated by FT-IR spectroscopy. As shown in Fig. 3(d), a signal at 1073 cm^{-1} was observed in the IR spectrum recorded for a poly(BA-a) composite filled with 0.5 wt% of nano-SiO_2 and attributed to asymmetric stretching of the Si–O–C groups formed upon condensation of the two components. Similar results were reported by Dueramae at al. [42] who observed signals at 1075 cm^{-1} upon mixing polybenzoxazines and nanosilica particles and attributed the absorptions to Si–O–C stretching frequencies. They also suggested that the interaction between polybenzoxazine and nanosilica could enhance its mechanical and thermal properties. Collectively, these results reflected an interaction between the poly(BA-a) and the incorporated nano-SiO_2. A possible chemical reaction between the BA-a resin and nano-SiO_2 is shown in Fig. 4. It was suggested that

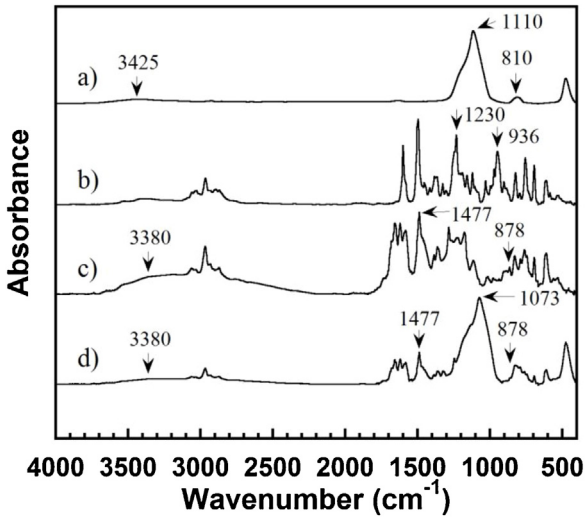

Fig. 3 – FTIR spectra recorded for the (a) nano-SiO_2, (b) benzoxazine monomer, (c) polybenzoxazine, and a (d) polybenzoxazine composite filled with nano-SiO_2 (0.5 wt%).

the BA-a oxazine ring was opened by thermal curing (Fig. 4(a)). The phenolic moiety of the ring opened the BA-a resin then reacted with hydroxyl group of nano-SiO_2 to form the Si–O–C linkages in the polymer networks as proposed in Fig. 4(b). The results suggested that the interaction between poly(BA-a) and nano-SiO_2 could occur in the nanocomposites.

3.2. *Tensile properties of S-glass fabric reinforced poly(BA-a) composites filled with nano-SiO_2*

The tensile properties of the fiber reinforced polymer composites are important parameters that affect the damage patterns and penetration depths experienced by composite panels under ballistic impact. The effect of added nano-SiO_2 on the tensile properties exhibited by S-glass fabric reinforced poly(BA-a) composites was investigated. As summarized in Fig. 5, the tensile strength value of the S-glass fabric reinforced poly(BA-a) composite was measured to be 328 MPa. The value increased to 437 MPa when up to 1.0 wt% of nano-SiO_2 was added; however, the use of quantities beyond 1.0 wt% had detrimental effects. The enhancement may stem from a uniform dispersion as well as strong interfacial bonding between the nano-SiO_2 and the poly(BA-a) matrix. In contrast, the decrease in the strength values at higher nanosilica loadings might pertain to a non-uniform dispersion and/or the formation of aggregates that become brittle under high strain in a manner that concentrates stress or initiates cracks. Regardless, the S-glass fabric reinforced poly(BA-a) composite filled with nano-SiO_2 exhibited a higher tensile strength value than that of E-glass fabric reinforced epoxy composites filled with

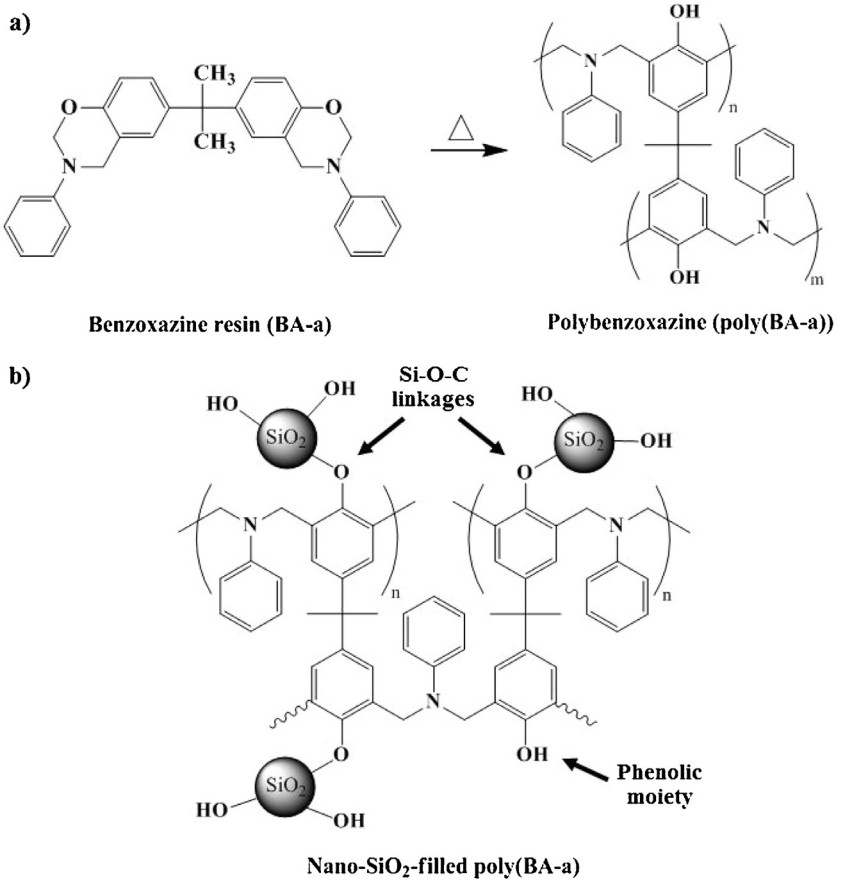

Fig. 4 – Summary of key chemical structures, including a) thermally induced polymerization benzoxazine and b) proposed chemical bonding between a polymer resin and nano-SiO_2.

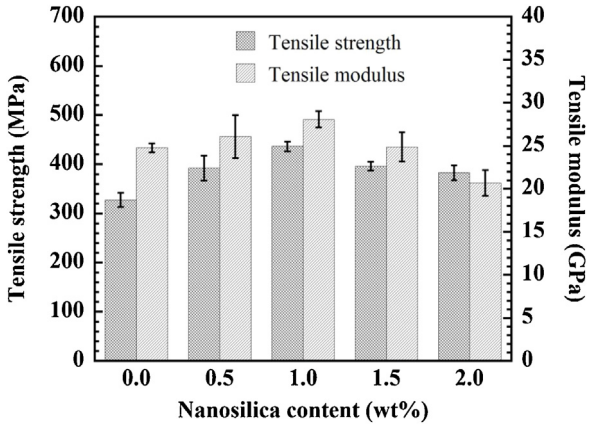

Fig. 5 – A summary of tensile properties exhibited by S-glass fabric reinforced poly(BA-a) composites filled with various quantities of nano-SiO_2 (indicated).

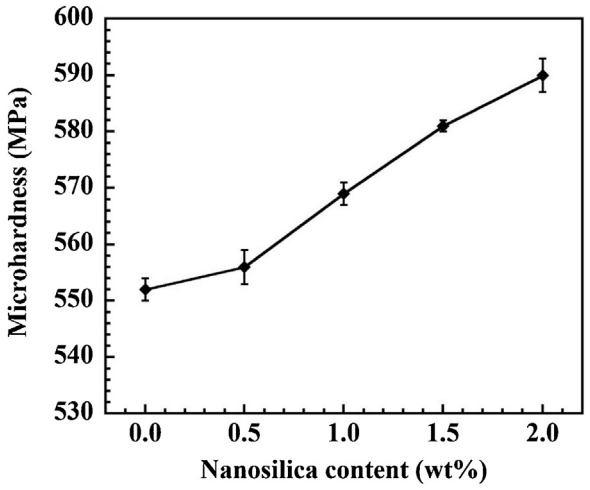

Fig. 6 – Microhardness of S-glass fabric reinforced poly(BA-a) composites filled with nano-SiO_2 vs. nano-SiO_2 content (indicated).

carboxyl functionalized multi-walled carbon nanotubes (c.f., 267 MPa) reported by Naghizadeh et al. [49].

The tensile modulus values of the S-glass fabric reinforced poly(BA-a) composites were also found to increase with added nano-SiO_2. For example, values ranging from 26.1 to 28.1 GPa were measured for poly(BA-a) composites containing 0.5–1.0 wt% of nano-SiO_2. For comparison, the tensile modulus value of an S-glass fabric reinforced poly(BA-a) composite that lacked nano-SiO_2 was measured to at 24.8 GPa. As before, the use of greater nano-SiO_2 loadings (1.5–2.0 wt%) decreased the measured tensile modulus values (24.9–20.7 GPa). We surmise that the rigidity of the nano-SiO_2 enhanced the stiffness of the composites up until a point where aggregates started to form and comprised the mechanical properties. The results implied that the incorporation of nano-SiO_2 into the fiber composite could improve tensile modulus of the nanocomposites when compared to that of the composites. Similar results were reported by Ramdani et al. [50] who showed that polybenzoxazine composites exhibited enhanced tensile moduli upon being mixed with silicon nitride. Moreover, S-glass fabric reinforced poly(BA-a) filled with 1.0 wt% of nano-SiO_2 showed the highest tensile properties especially tensile modulus which influenced on the ballistic behavior in term of damage pattern and depth of penetration.

3.3. *Microhardness of S-glass fabric reinforced poly(BA-a) composites filled with nano-SiO_2*

Microhardness is also an important factor that affects ballistic management and rigid fillers are often utilized to enhance pertinent characteristics. As shown in Fig. 6, the microhardness of nano-SiO_2-filled poly(BA-a) composites reinforced with S-glass fabric substantially increased with added nano-SiO_2. For example, the hardness of a S-glass fabric reinforced poly(BA-a) composite was measured to be 552 MPa. However, the value increased to 556, 569, 581 and 590 MPa upon the addition of 0.5, 1.0, 1.5, and 2.0 wt% of nano-SiO_2, respectively. The enhancement was attributed to the high hardness value of the nanosilica particles (10.8 GPa). The uniform dispersion of the nanosilica particles in the poly(BA-a) matrix as well as strong chemical interactions between the nanosilica particles and the poly(BA-a) matrix may also be key contributors. As revealed previously by FTIR spectroscopy, the nanosilica particles formed covalent bonds with the poly(BA-a) through Si–O–C linkages resulting in good interfacial adhesion between the nanosilica and the poly(BA-a) matrix.

3.4. *Morphology of S-glass fabric reinforced poly(BA-a) composites filled with nano-SiO_2*

A scanning electron microscope (SEM) was used to visualize the dispersions of the nano-SiO_2 particles in the poly(BA-a) matrix. Fig. 7 shows SEM images that were recorded for pristine nano-SiO_2, poly(BA-a), S-glass fabric and S-glass fabric reinforced poly(BA-a) composites filled with nano-SiO_2 (1.0 wt%). Agglomerates were observed in the pristine nano-SiO_2 as shown in Fig. 7(a) which may stem from the intermolecular interaction of hydroxyl groups present on their hydrophilic surface (see above). A smooth, fractured surface was observed upon inspection of the image recorded for the poly(BA-a) which may be due to the brittle nature of the material as seen in Fig. 7(b). The S-glass fabric appeared to be relative smooth and free of defects, and featured cylinders with diameters in the range of 12 μm (Fig. 7(c)). The image recorded for a composite filled with 1.0 wt% of nano-SiO_2 indicated that the material was relatively uniform: the nano-SiO_2 was well dispersed in the poly(BA-a) matrix with good interfacial adhesion between the two components (see Fig. 7(d)), a result that rationalizes the enhanced tensile properties exhibited by the composites.

The fracture surface of a S-glass fabric reinforced poly(BA-a) composite filled with 1.0 wt% of nano-SiO_2 was also studied by SEM; warp and weft regions are shown in Fig. 8(a) and Fig. 8(b), respectively. As gleaned from the data, the pull-out length of the S-glass fabric is shorter than its full length, which indicated that the S-glass fabric was adhered to the poly(BA-a) matrix. Indeed, pieces of the matrix were observed to be attached to the fiber. Moreover, the fracture surface was found

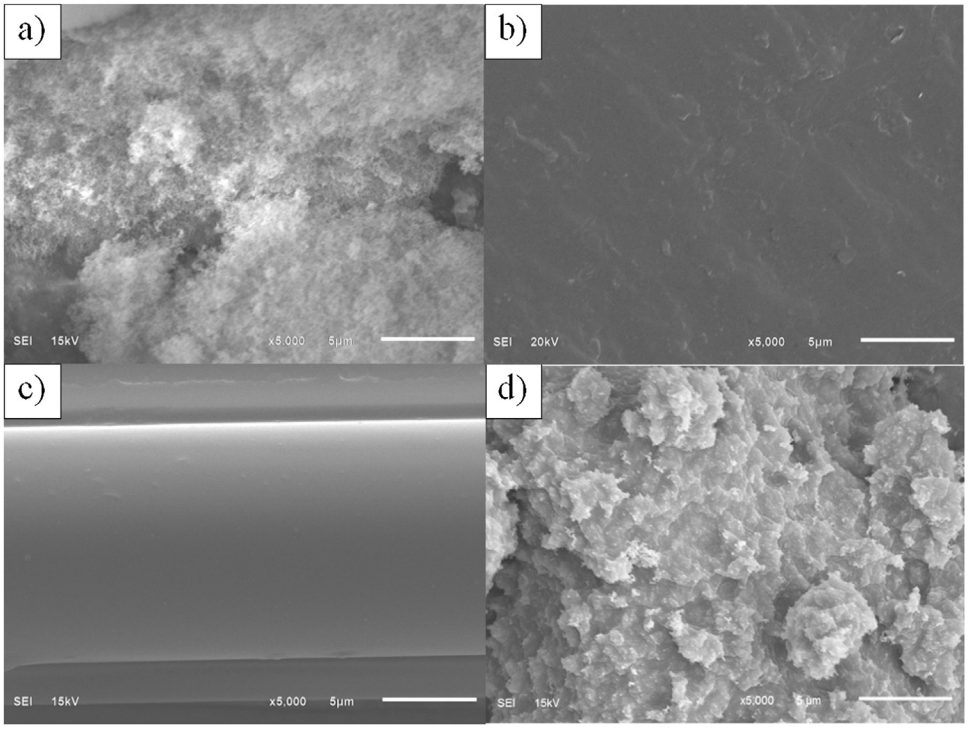

Fig. 7 – SEM images of (a) pristine nano-SiO_2, (b) poly(BA-a), (c) S-glass fabric and a (d) S-glass fabric reinforced poly(BA-a) composite filled with nano-SiO_2 (1.0 wt%) as recorded at 5000x magnification.

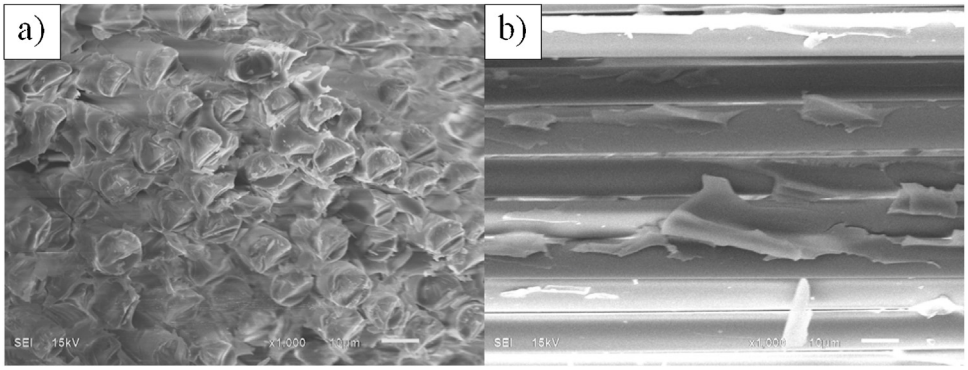

Fig. 8 – SEM images of the (a) warp and (b) weft regions of S-glass fabric reinforced poly(BA-a) composites filled with 1.0 wt% of nano-SiO_2 as recorded at 1000x magnification.

to be embedded which suggested to us that cohesive failure occurred due to good interfacial adhesion between the polymer matrix, filler and fiber, and provided additional support for the enhanced mechanical properties exhibited by the composite.

3.5. *Ballistic performance of multilayered armor based on polybenzoxazine composites*

A series of ballistic impact tests was performed on armor specimens fabricated using 35-ply S-glass fabric reinforced poly(BA-a) composites as strike panels and backed by an aramid fabric composite. Some of the composites used to fabricate the strike panels were filled with nano-SiO_2 (1 wt%) whereas others were unfilled. Selected areas ($150 \times 150\,mm^2$) were subjected to 5.56×45 mm projectiles with impact velocities of 920 ± 30 m/s. As shown in Fig. 9, the impact velocity of the unfilled composite was measured at 897 m/s whereas the impact velocity of the filled composite was 913 m/s. Although the strike panels were perforated, the back panels were only partially penetrated and, as such, it appeared that both specimens could potentially stop and catch the projectiles. Inspection of the photographs taken after the ballistic tests indicated that the major failure mechanism exhibited by the specimens used in the strike panels was fiber breakage and matrix cracking. The diameter of the damaged area on the impacted side of the strike panel containing the composite filled with nano-SiO_2 was measured to be 51 mm, which

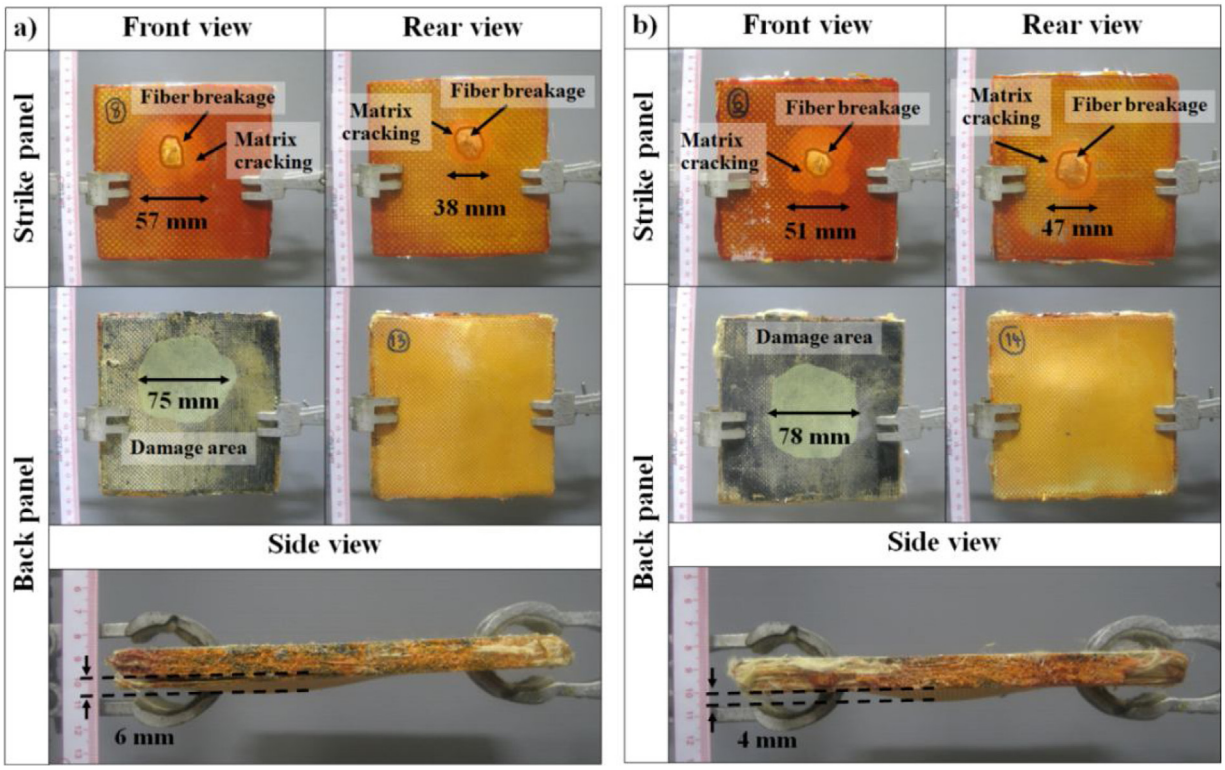

Fig. 9 – Photographs of strike panel specimens made from of S-glass fabric reinforced poly(BA-a) that was either (a) unfilled or (b) filled with nano-SiO_2 and after being impacted with a 5.56 × 45 mm projectile. The back panels consisted of aramid fabric composite.

was 10.5% lower than the diameter of the damage (57 mm) measured for the strike panel made from an unfilled composite. The difference may be explained by the respective tensile moduli: the composite filled with nanosilica had 13.3% greater tensile modulus (28.1 GPa) than that of the unfilled composite (24.8 GPa). Thus, the S-glass fabric reinforced polybenzoxazine composite filled with nano-SiO_2 could withstand a higher tension force before failure which resulted in superior ballistic performance in terms of reduction in damage area. Likewise, the nano-SiO_2 filler dispersed in the polymer matrix may act as a barrier to crack propagation and facilitate the absorption of energy upon impact.

The diameter of the damaged area on the rear side of the strike panel made of the composite filled with nano-SiO_2 was measured to 47 mm, which was greater than that measured for the analogous damaged area (38 mm) on the strike panel made from the unfilled composite. Likewise, different cone formation diameters were measured on the rear sides of the back panels (78 mm vs. 75 mm, respectively). The difference may depend on the abilities of the panels to absorb energy. Moreover, as can be seen from side views of the impacted back panels, approximately 33% lower penetration depths were measured when the strike panel composites were filled with nano-SiO_2 as compared to panels that lacked the filler (4 mm vs. 6 mm, respectively). The difference may be due to the higher hardness of the filled composites which effectively fragment the projectile and significantly reduce the impacted energy. Collectively, the results indicated that the filled composites may be suitable for use in multilayered hard armor applications, especially considering that the areal weight density of the filled composite was measured to be 5.13 g/cm^2.

3.6. *Numerical simulation analyses of multilayered armor based on polybenzoxazine composites and a comparison of the experimental and numerical results*

As illustrated in Fig. 10, a series of numerical simulations were performed to assess the projectile penetration processes. Key material properties are summarized in Table 3. The material properties of the back panels were adopted from a report by Okhawilai et al. [33]. Strike panel fracture occurs as the projectile penetrates the first layer, which requires approximately 13 μs. For comparison, the back panel begins to fail at approximately 25 μs after impact with continuing damage occurring over a period of 43–340 μs, indicating that stress waves propagate even if the projectile reaches the back panel. The projectile stops moving at 490 μs.

The numerical ballistic impact simulation results were compared to the experimental data in terms of the damage areas on the front and rear sides of the tested panels. As shown in Fig. 11, the numerical simulation model qualitatively predicted the non-uniform shape of the perforation. The extent of damage area experienced by the strike panel was measured to be 49 mm × 51 mm, while the predicted damage area was 51 mm × 49 mm with an overall difference of approximately 4%. The extent of perforation was experimentally measured to be 21 mm in diameter whereas the numerical simulation model predicted a diameter of 20 mm, a difference of approx-

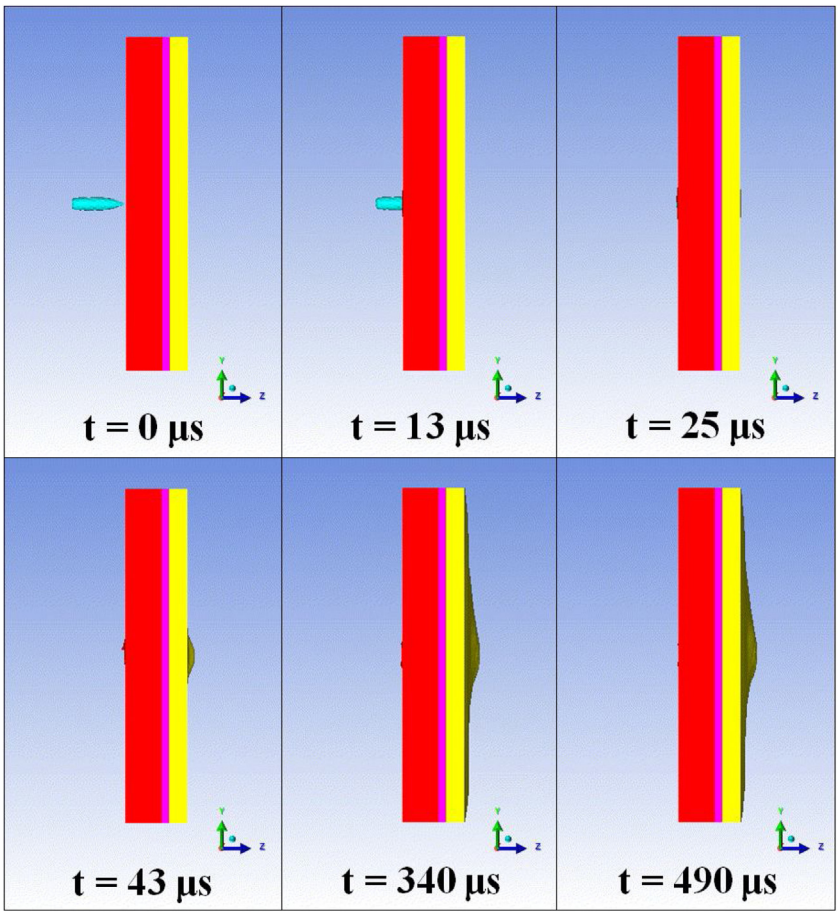

Fig. 10 – A summary of numerical simulation analyses that were performed on polybenzoxazine composites undergoing ballistic impact over different periods of times (indicated).

Table 3 – A summary of materials properties exhibited by the multilayered composites.

Properties		1st layer (strike panel)[a]	2nd layer (back panel)[b]	3rd layer (back panel)[c]
Thickness, mm		16.4	3.0	8.5
Density, g/cm^3		2.3	1.6	1.5
Young modulus, kPa	E_{11}	7.5×10^7	2.5×10^7	2.3×10^7
	E_{22}	7.5×10^7	2.5×10^7	2.3×10^7
	E_{33}	7.5×10^6	1.7×10^6	1.5×10^6
Poisson's ratio	ν_{12}	0.12	0.07	0.07
	ν_{23}	0.4	0.698	0.698
	ν_{31}	0.2	0.075	0.075
Strength: Shear modulus, kPa	G_{12}	4×10^5	4×10^5	3×10^5
	G_{23}	4.1×10^4	1.7×10^4	1.5×10^4
	G_{31}	4.1×10^4	1.7×10^4	1.5×10^4
Failure: Tensile failure stress or strain	σ_{11} or ϵ_{11}	7.1×10^5	0.07	0.07
	σ_{22} or ϵ_{22}	7.1×10^5	0.07	0.07
	σ_{33} or ϵ_{33}	7×10^4	0.02	0.02

[a] 1st layer refers to a S-glass fabric reinforced poly(BA-a) composite filled with nano-SiO_2.
[b] 2nd layer refers to an aramid fabric reinforced poly(BA-a/PU) composite filled with MWCNTs.
[c] 3rd layer refers to an aramid fabric reinforced poly(BA-a/PU) composite.

imately 5%. Similar congruence between the simulations and the experimental data were also observed for the back panels. For example, the extent of damage found in the back panel was experimentally measured to be 27 mm × 29 mm while the predicted area was 27 mm × 25 mm, a difference of approximately 14%. In addition, good agreement between the experimental and simulated penetration depths was also observed. The experimental penetration depth was measured to be 4 mm (Fig. 9(b)) whereas the numerical simulation model predicted a perforation depth of 4.5 mm (Fig. 11(e)), a difference of approx-

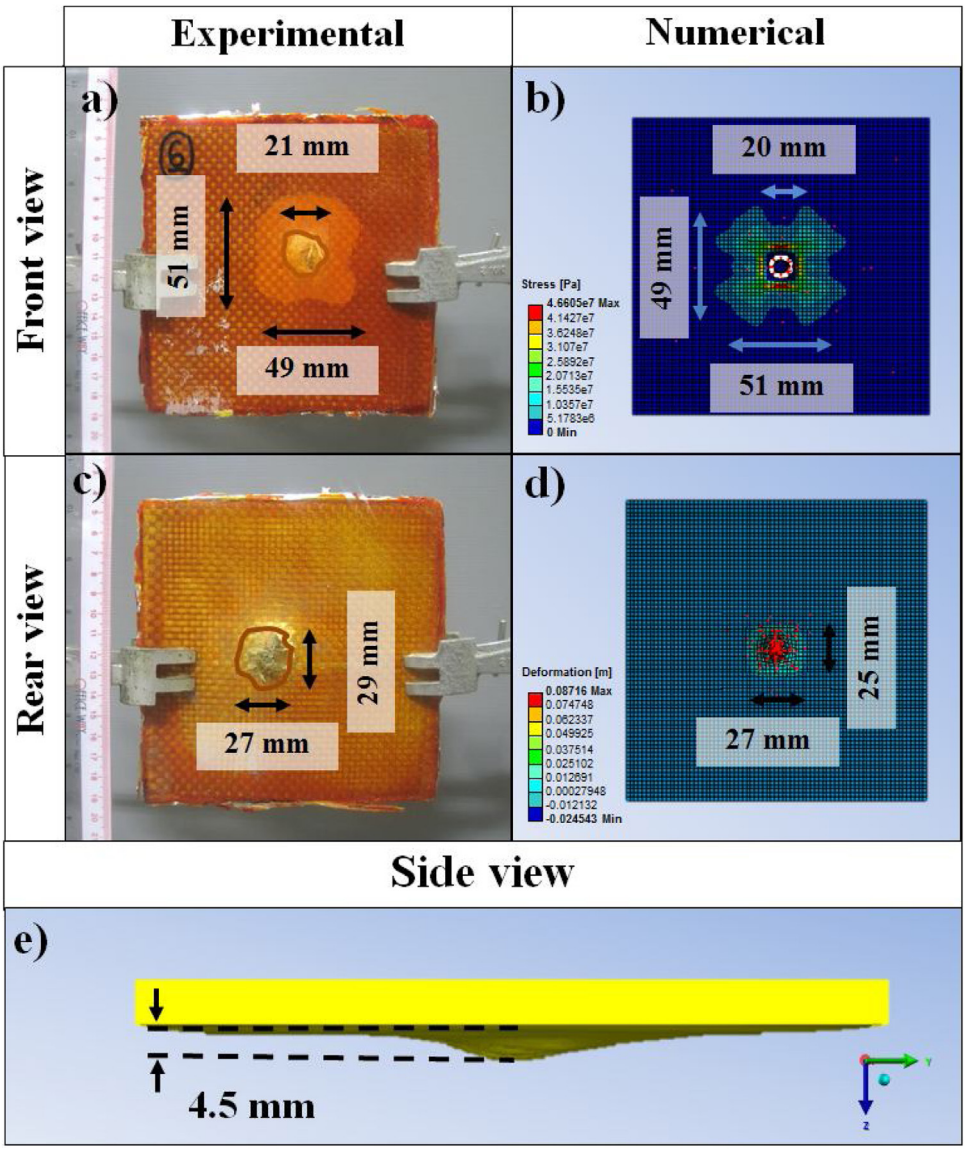

Fig. 11 – Comparison of the experimental and numerical damaged areas exhibited by strike panels that were made from polybenzoxazine composites and after being impacted.

imately 12.5%. Likewise, the patterns of the experimental and simulated deformations were qualitatively similar.

3.7. *Ballistic performance predicted by numerical simulation of multilayered armor based on polybenzoxazine composites*

Numerical simulations were used to predict the ballistic impact performance of multilayered armor that consisted of strike panels made from S-glass fabric reinforced poly(BA-a) filled with nano-SiO_2 and back panels made from an aramid fabric composite; key results are shown in Fig. 12. The main objectives of the numerical simulations were to predict the suitable thickness of the strike panel at a maximum impact velocity of 950 m/s and to reduce the overall weight of the armor. Inspection of the numerical data indicated that the specimens with strike panel thicknesses between 14.8 mm and 16.4 mm could potentially stop and catch 5.56×45 mm projectiles without penetrating the back panel. In other words, effective stress transfer between thicker plies could provide increased ballistic protection. The limit may be 13.1 mm as multilayered armor with such a thickness may not protect against 5.56×45 mm projectiles with an impact velocity of 950 m/s as indicated by the data. Regardless, the depth of penetration of the armor is predicted to be less than 44 mm as required by the standard.

Critical ballistic performance parameters, including the ballistic limit velocity (V_{50}) and energy absorption (E_{Abs}), were also simulated. The V_{50} was evaluated by varying the impact velocity and an average of the highest partial perforation velocities and the lowest full perforation velocity. The impact velocity started at 900 m/s and increased in 50 m/s increments. As shown in Fig. 13, the velocity average was used to derive the ballistic limit velocity, which was predicted to 1075 m/s.

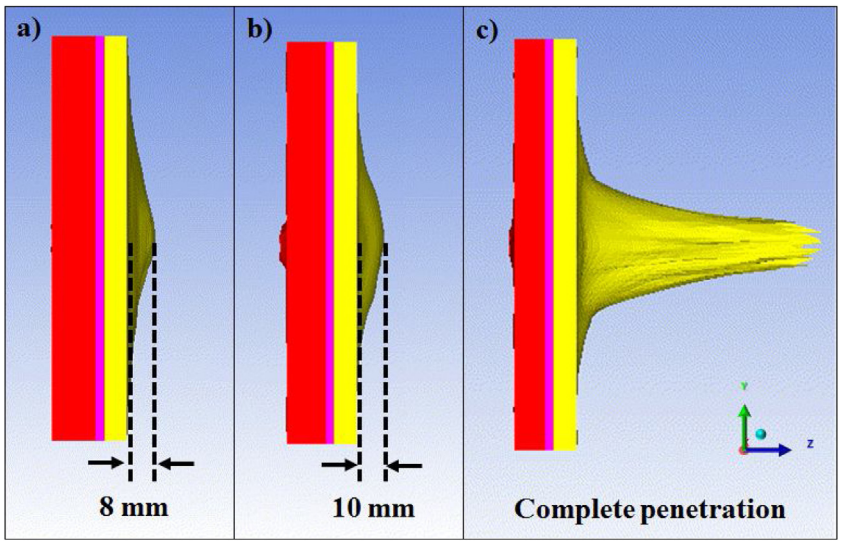

Fig. 12 – Simulated penetration depth exhibited by polybenzoxazine composites with various strike panel thicknesses (indicated).

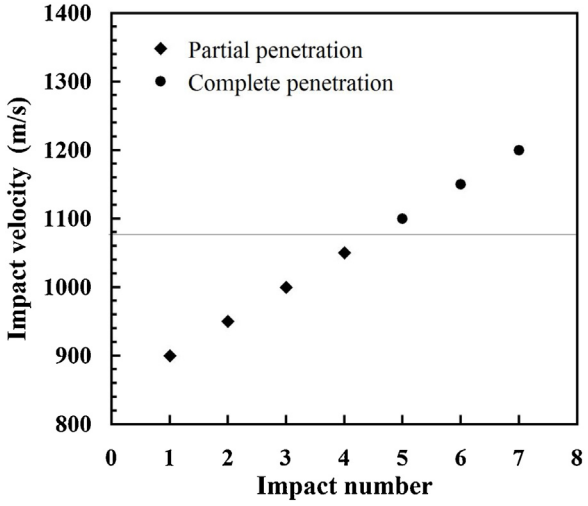

Fig. 13 – Impact velocity vs. impact number for a polybenzoxazine composite that was impacted by a 5.56 x 45 mm projectile.

Lee and Yoo [51] used similar methodology to calculate a V_{50} of ceramic/metal composite armor (750 m/s; areal weight density of 5.0 g/cm^2) using 7.62 mm armor piercing projectiles. The estimated E_{Abs} of the polybenzoxazine based composites was calculated to be as high as 2311 J using Eq. (1). Collectively, the results indicated that multilayered hard armor could protect against the perforation of 5.56 × 45 mm projectiles with impact velocities of 920 ± 30 m/s.

4. Conclusions

The effect of added nano-SiO_2 on the mechanical properties and ballistic impact response of S-glass fabric reinforced polybenzoxazine composites was successfully investigated. The mechanical, i.e. strength and modulus under tension and hardness of the poly(BA-a) nanocomposites were found to be substantially improved upon the addition of nano-SiO_2. Likewise, the high tensile moduli of the strike panels based on polybenzoxazine nanocomposites could result in a superior ballistic impact response particularly in terms of both reduction in back face deformation and depth of penetration on rear side of the back panel. Moreover, hardness of the strike panel indicated to an ability to destroy the projectile into fragment with no failure was formed on the back panel. A series of numerical simulations were used to predict the damage with relatively low error and good correlation with the experimental data. Moreover, the V_{50} and E_{Abs} values of the composites were predicted to be as high as 1075 m/s and 2311 J, respectively. Hard armor specimen based on S-glass fabric reinforced poly(BA-a) composites filled with 1.0 wt% of nano-SiO_2 protected against the perforation of 5.56 × 45 mm projectiles with velocities of 950 ± 30 m/s. Collectively, the results indicated that these composites are poised for use as strike panels in multilayered hard armor applications.

Conflicts of interest

The authors declare no conflicts of interest.

Acknowledgement

The authors acknowledge financial support from the Royal Golden Jubilee (RGJ) Ph.D. Program (Grant No. PHD/0177/2560) under the Thailand Research Fund (TRF), Thailand and the 90th Anniversary of Chulalongkorn University, (Ratchadaphiseksomphot Endowment Fund). The Defense Science and Technology Department (DSTD), Thailand is also acknowledged for specimen testing. CWB acknowledges the IBS (IBS-R019-D1) for support.

Appendix A. Supplementary data

Supplementary material related to this article can be found, in the online version, at doi:https://doi.org/10.1016/j.jmrt.2020.09.005.

REFERENCES

[1] Domun N, Kaboglu C, Paton KR, Dear JP, Liu J, Blackman BRK, et al. Ballistic impact behaviour of glass fibre reinforced polymer composite with 1D/2D nanomodified epoxy matrices. Compos Part B-Eng 2019;167:497–506.

[2] Okhawilai M, Rimdusit S. Chapter 35 - Hard armor composites from ballistic fiber-reinforced polybenzoxazine alloys A2 - ishida, hatsuo. In: Froimowicz P, editor. Advanced and emerging polybenzoxazine science and technology. Amsterdam: Elsevier; 2017. p. 699–723.

[3] Clifton S, Thimmappa BHS, Selvam R, Shivamurthy B. Polymer nanocomposites for high-velocity impact applications-A review. Compos Commun 2020;17:72–86.

[4] Braga Fd O, Milanezi TL, Monteiro SN, Louro LHL, Gomes AV, Lima ÉP. Ballistic comparison between epoxy-ramie and epoxy-aramid composites in Multilayered Armor Systems. J Mater Res Technol 2018;7:541–9.

[5] Benzait Z, Trabzon L. A review of recent research on materials used in polymer–matrix composites for body armor application. J Compos Mater 2018;52:3241–63.

[6] Monteiro SN, Milanezi TL, Louro LHL, Lima ÉP, Braga FO, Gomes AV, et al. Novel ballistic ramie fabric composite competing with Kevlar™ fabric in multilayered armor. Mater Des 2016;96:263–9.

[7] U.S. Department of Justice. Office of justice program, national institute of justice, ballistic resistance of body armor NIJ 0101.06; 2008.

[8] Coghe F, Nsiampa N, Rabet L, Dyckmans G. Experimental and numerical investigations on the origins of the bodywork effect (K-Effect). J Appl Mech 2010;77:051801.

[9] Bracamonte L, Loutfy R, Yilmazcoban IK, Rajan SD. 12 - Design, manufacture, and analysis of ceramic-composite armor A2 - Bhatnagar, Ashok. Lightweight Ballistic Composites (Second Edition). Woodhead Publishing; 2016. p. 349–67.

[10] Garcia Filho FDC, Oliveira MS, Pereira AC, Nascimento LFC, Ricardo Gomes Matheus J, Monteiro SN. Ballistic behavior of epoxy matrix composites reinforced with piassava fiber against high energy ammunition. J Mater Res Technol 2020;9:1734–41.

[11] Tepeduzu B, Karakuzu R. Ballistic performance of ceramic/composite structures. Ceram Int 2019;45:1651–60.

[12] JLd Santos, Marçal RLSB, PRRd Jesus, Gomes AV, Lima ÉP, Navarro da Rocha D, et al. Mechanical properties and ballistic behavior of LiF-added Al2O3–4wt%Nb2O5 ceramics. J Mater Res Technol 2018;7:592–7.

[13] Crouch IG, Appleby-Thomas G, Hazell PJ. A study of the penetration behaviour of mild-steel-cored ammunition against boron carbide ceramic armours. Int J Impact Eng 2015;80:203–11.

[14] Yin Z, Yuan J, Chen M, Si D, Xu C. Mechanical property and ballistic resistance of graphene platelets/B4C ceramic armor prepared by spark plasma sintering. Ceram Int 2019;45:23781–7.

[15] Makeev MA, Srivastava D. Molecular dynamics simulations of hypersonic velocity impact protection properties of CNT/a-SiC composites. Compos Sci Technol 2008;68:2451–5.

[16] Crouch IG, Kesharaju M, Nagarajah R. Characterisation, significance and detection of manufacturing defects in Reaction Sintered Silicon Carbide armour materials. Ceram Int 2015;41:11581–91.

[17] Zheng JQ, Walsh SM. 14 - Materials, manufacturing, and enablers for future soldier protection A2 - Bhatnagar, Ashok. Lightweight Ballistic Composites (Second Edition). Woodhead Publishing; 2016. p. 393–437.

[18] FSd Assis, Pereira AC, Filho Fd CG, Lima ÉP, Monteiro SN, Weber RP. Performance of jute non-woven mat reinforced polyester matrix composite in multilayered armor. J Mater Res Technol 2018;7:535–40.

[19] Braga Fd O, Bolzan LT, Lima Jr ÉP, Monteiro SN. Performance of natural curaua fiber-reinforced polyester composites under 7.62mm bullet impact as a stand-alone ballistic armor. J Mater Res Technol 2017;6:323–8.

[20] Braga Fd O, Bolzan LT, FSd Luz, Lopes PHLM, Lima Jr ÉP, Monteiro SN. High energy ballistic and fracture comparison between multilayered armor systems using non-woven curaua fabric composites and aramid laminates. J Mater Res Technol 2017;6:417–22.

[21] dos Santos Alves AL, Cassiano Nascimento LF, Suarez JCM. Influence of weathering and gamma irradiation on the mechanical and ballistic behavior of UHMWPE composite armor. Polym Test 2005;24:104–13.

[22] Wang H, Hazell PJ, Shankar K, Morozov EV, Escobedo JP. Impact behaviour of Dyneema® fabric-reinforced composites with different resin matrices. Polym Test 2017;61:17–26.

[23] Ansari MM, Chakrabarti A. Influence of projectile nose shape and incidence angle on the ballistic perforation of laminated glass fiber composite plate. Compos Sci Technol 2017;142:107–16.

[24] Chinnasamy V, Pavayee Subramani S, Palaniappan SK, Mylsamy B, Aruchamy K. Characterization on thermal properties of glass fiber and kevlar fiber with modified epoxy hybrid composites. J Mater Res Technol 2020.

[25] Tang E, Zhang X, Han Y. Experimental research on damage characteristics of CFRP/aluminum foam sandwich structure subjected to high velocity impact. J Mater Res Technol 2019;8:4620–30.

[26] Ishida H. Process for preparation of benzoxazine compounds in solventless systems, US patent no.5543516; 1996.

[27] Ghosh NN, Kiskan B, Yagci Y. Polybenzoxazines—new high performance thermosetting resins: synthesis and properties. Prog Polym Sci 2007;32:1344–91.

[28] Takeichi T, Guo Y, Agag T. Synthesis and characterization of poly(urethane-benzoxazine) films as novel type of polyurethane/phenolic resin composites. J Polym Sci: Polym Chem Ed 2000;38:4165–76.

[29] Ishida H, Allen DJ. Physical and mechanical characterization of near-zero shrinkage polybenzoxazines. J Polym Sci: Polym Phys Ed 1996;34:1019–30.

[30] Rimdusit S, Jubsilp C, Tiptipakorn S. Alloys and composites of polybenzoxazines: properties and applications. New York: Springer; 2013.

[31] Ishida H, Agag T. Handbook of benzoxazine resins. Elsevier; 2011.

[32] Gopinath G, Zheng JQ, Batra RC. Effect of matrix on ballistic performance of soft body armor. Compos Struct 2012;94:2690–6.

[33] Okhawilai M, Hiziroglu S, Rimdusit S. Measurement of ballistic impact performance of fiber reinforced polybenzoxazine/polyurethane composites. Measurement 2018;130:198–210.

[34] Jajam KC, Tippur HV. Quasi-static and dynamic fracture behavior of particulate polymer composites: a study of nano-

vs. Micro-size filler and loading-rate effects. Compos Part B-Eng 2012;43:3467–81.
[35] Pandya KS, Akella K, Joshi M, Naik NK. Ballistic impact behavior of carbon nanotube and nanosilica dispersed resin and composites. J Appl Phys 2012;112:113522.
[36] Naqi A, Abbas N, Zahra N, Hussain A, Shabbir SQ. Effect of multi-walled carbon nanotubes (MWCNTs) on the strength development of cementitious materials. J Mater Res Technol 2019;8:1203–11.
[37] Zare Y, Rhee KY. Analysis of critical interfacial shear strength between polymer matrix and carbon nanotubes and its impact on the tensile strength of nanocomposites. J Mater Res Technol 2020.
[38] Pol MH, Liaghat GH, Hajiarazi F. Effect of nanoclay on ballistic behavior of woven fabric composites: experimental investigation. J Compos Mater 2012;47:1563–73.
[39] Sivanjineyulu V, Behera K, Chang YH, Chiu FC. Selective localization of carbon nanotube and organoclay in biodegradable poly(butylene succinate)/polylactide blend-based nanocomposites with enhanced rigidity, toughness and electrical conductivity. Compos Part A-Appl S 2018;114:30–9.
[40] Zare Y, Rhee KY. Tensile modulus prediction of carbon nanotubes-reinforced nanocomposites by a combined model for dispersion and networking of nanoparticles. J Mater Res Technol 2020;9:22–32.
[41] He P, Huang M, Yu B, Sprenger S, Yang J. Effects of nano-silica contents on the Properties of epoxy nanocomposites and Ti-epoxy assembles. Compos Sci Technol 2016;129:46–52.
[42] Dueramae I, Jubsilp C, Takeichi T, Rimdusit S. High thermal and mechanical properties enhancement obtained in highly filled polybenzoxazine nanocomposites with fumed silica. Compos Part B-Eng 2014;56:197–206.
[43] Zhang R, Han B, Li L, Zhao Z-N, Zhang Q, Zhang Q, et al. Influence of prestress on ballistic performance of bi-layer ceramic composite armors: experiments and simulations. Compos Struct 2019;227:111258.
[44] Miranda P, Pajares A, Meyers MA. Bioinspired composite segmented armour: numerical simulations. J Mater Res Technol 2019;8:1274–87.
[45] Okhawilai M, Parnklang T, Mora P, Hiziroglu S, Rimdusit S. The energy absorption enhancement in aramid fiber-reinforced poly(benzoxazine-co-urethane) composite armors under ballistic impacts. J Reinf Plast Compos 2019;38:133–46.
[46] Ishida H. Process for preparation of benzoxazine compounds in solventless systems. In: US Pat. 5, 516 (1996). Editor; 1996.
[47] Mora P, Koschek K, Rimdusit S. Development of high performance multilayered armor based on polybenzoxazine nanocomposites. Submission to Polym Compos 2020.
[48] ANSYS AUTODYN Library Version 16.
[49] Naghizadeh Z, Faezipour M, Pol MH, Liaghat GH, Abdolkhani A. Improvement in impact resistance performance of glass/epoxy composite through carbon nanotubes and silica nanoparticles. Proc Inst Mech Eng Part L J Mater Des Appl 2016;232:785–99.
[50] Ramdani N, Wang J, Wang H, T-t Feng, Derradji M, Liu W-b. Mechanical and thermal properties of silicon nitride reinforced polybenzoxazine nanocomposites. Compos Sci Technol 2014;105:73–9.
[51] Lee M, Yoo YH. Analysis of ceramic/metal armour systems. Int J Impact Eng 2001;25:819–29.